Probing the Accretion Processes in Soft X-Ray Selected Polars

I. Traulsen[1], K. Reinsch[2], A. D. Schwope[1]

[1] *Leibniz-Institut für Astrophysik Potsdam (AIP), An der Sternwarte 16, 14482 Potsdam, Germany*

[2] *Institut für Astrophysik, Georg-August-Universität Göttingen, Friedrich-Hund-Platz 1, 37077 Göttingen, Germany*

Corresponding author: **itraulsen@aip.de**

Abstract

High-energy data of accreting white dwarfs give access to the regime of the primary accretion-induced energy release and the different proposed accretion scenarios. We perform XMM-Newton observations of polars selected due to their ROSAT hardness ratios close to -1.0 and model the emission processes in accretion column and accretion region. Our models consider the multi-temperature structure of the emission regions and are mainly determined by mass-flow density, magnetic field strength, and white-dwarf mass. To describe the full spectral energy distribution from infrared to X-rays in a physically consistent way, we include the stellar contributions and establish composite models, which will also be of relevance for future X-ray missions. We confirm the X-ray soft nature of three polars.

Keywords: cataclysmic variables - polars - spectroscopy - photometry - X-rays - individual: AI Tri, QS Tel, RS Cae.

1 Introduction

Accretion onto magnetic white dwarfs involves plasma under extreme physical conditions, in particular high temperatures up to millions of Kelvin. X-ray observations of the discless AM Her-type systems ("polars") provide direct insight into the accretion processes and the opportunity to study related system properties. Hard X-ray emission ($E > 0.5\,\text{keV}$) arises from the cooling accretion column above the white dwarf and soft ($E < 0.5\,\text{keV}$) from the heated accretion region on the white-dwarf surface. Model calculations and recent spectral analyses reveal complex structures of the emission regions and a wide range of temperatures and densities.

Several systems are found at excesses of soft over hard X-ray flux by factors up to $1\,000$, which can be interpreted as a sign of inhomogeneous accretion. Full understanding of the accretion processes and the binary system requires multi-wavelength data, since the different system components dominate the spectral energy distribution (SED) at different wavelengths from infrared up to X-rays.

In a campaign of dedicated XMM-Newton and optical observations of selected AM Her-type systems, we spectrophotometrically study the parameters and flux contributions of their components. We concentrate on the conditions in the emission regions in the post-shock accretion column and on the heated white dwarf, flux and luminosity ratios and their strong dependence on the choice of the underlying spectral models. Here, we summarize our work on three soft X-ray selected polars and our efforts to establish consistent multi-wavelength models.

2 Observed SEDs

Starting in 2005, we obtained XMM-Newton X-ray and ultraviolet data of AI Tri, QS Tel, and RS Cae (obs. IDs 0306840901, 0306841001, 0404710401, 0554740801; Traulsen et al., 2010, 2011, 2014), covering one to five orbital cycles per object. On the basis of optical monitoring, the TOO observations were triggered during high and intermediate high states of accretion. Optical photometry and – for QS Tel – spectroscopy were performed (quasi)simultaneously. To construct the full long-term SEDs of the objects from infrared to X-ray wavelengths, we use publicly available archival data, in particular of the WISE, 2MASS, HST, FUSE, and ROSAT archives. Figure 1 shows all data, the main system components being marked according to their approximate flux maxima in the middle panel as follows: *a.* the secondary star in the IR, *b.* the cyclotron emission in the IR to optical, *c.* the accretion stream and *d.* the white-dwarf primary in the optical to UV, *e.* the accretion-heated region on the white-dwarf surface in the extreme UV to the soft X-ray regime, and *f.* the post-shock accretion column in hard X-rays. All panels include both high-state and low-state data, identifiable by their different flux levels. The distinct soft X-ray / EUV components at high states are clearly visible, compared for example to the low-state SED of EF Eri

(Schwope et al. 2007) or to the serendipitously discovered X-ray hard polar 2XMMp J131223.4+173659 (Vogel et al. 2008). At times of high soft X-ray flux, the optical and soft X-ray data show pronounced short-term variability ("flickering").
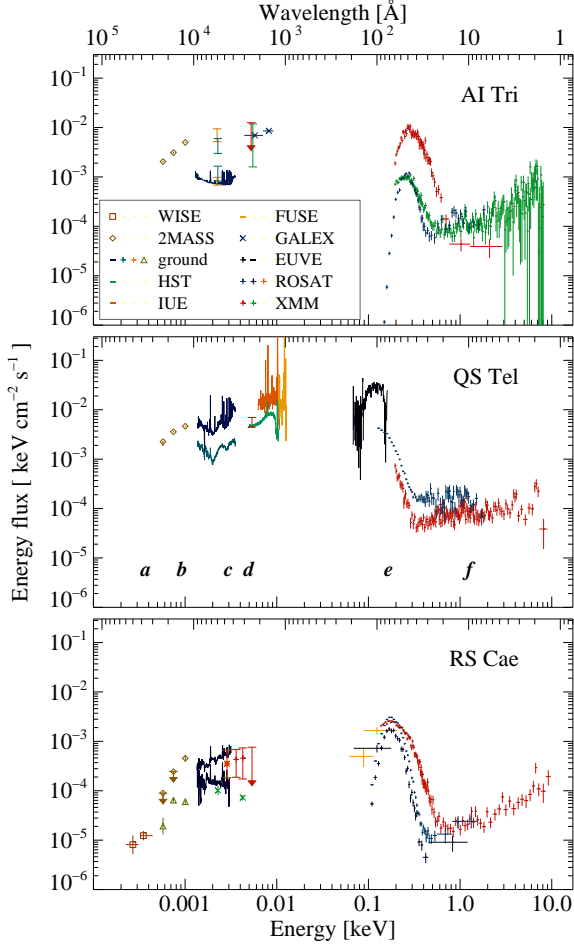

Figure 1: Observed SEDs of three X-ray soft polars from IR to X-rays: our XMM-Newton and optical plus archival data at different epochs and accretion states (cf. Traulsen et al. 2010, 2011, 2014). The X-ray spectra are unfolded using the best-fit models.

3 Multi-Wavelength Modeling

To consistently describe the spectral energy distribution and multi-band light curves, we synthesize spectral models for one uniform set of system parameters and calculate the corresponding light curves. For the different system components, we adopt (referring to the labels used in Sect. 2 and Fig. 1): *a.* a PHOENIX stellar atmosphere model of an M star (Hauschildt & Baron 1999), *b.* a cyclotron component of a stratified postshock accretion column (Fischer & Beuermann 2001), *c.* a simplified accretion-stream component of a 3D binary model (Staude et al. 2001), *d.* a non-LTE white-dwarf atmosphere model (Werner & Dreizler 1999), *e.* a single- or multi-temperature black body or hot white-dwarf atmosphere, *f.* a single- or multi-temperature plasma model of the accretion column.

The input parameters of the models are determined from observational data, where possible, and estimated as typical values for primary white dwarf and secondary M star otherwise (e.g. Townsley & Gaensicke 2009, Knigge 2006). In particular, orbital period, inclination, and magnetic field strength are available from optical spectroscopy and polarimetry; parameters of the accretion-induced emission are fitted to the X-ray spectra (cf. Sect. 4 and Table 1).

Table 1: Parameters of the best fits to the XMM-Newton spectra. Bolometric ROSAT flux ratios at fixed temperatures are calculated from [a]Schwarz et al. 1998, [b]Schwope et al. 1995, [c]Burwitz et al. 1996, applying corrections of $\kappa_{\mathrm{bb}} = 2.5$, $\kappa_{\mathrm{br}} = 4.8$.

	AI Tri	QS Tel	RS Cae
black body	multi-T	single-T	single-T
plasma model	multi-T	two-T	single-T
$N_{\mathrm{H,ISM}}$ [cm^{-2}]	$\sim 10^{20}$	$\sim 10^{20}$	$2 \pm 1 \times 10^{19}$
kT_{bbody} [eV]	44 ± 5	20 ± 4	36 ± 1
kT_{plasma} [keV]	$1 .. 20$	$0.2 .. 4.0$	7 ± 3
$N_{\mathrm{H,intr}}$ [cm^{-2}]	$3 \pm 2 \times 10^{23}$	$10^{22} .. 10^{23}$	$\sim 4 \times 10^{23}$
$\log \dot{M}$ [M$_\odot$/yr]	$-11 .. -9$	~ -10	~ -10
$F_{\mathrm{bb}}/F_{\mathrm{plasma}}$	$\sim 3 .. 200$	$\sim 10 .. 100$	~ 11
$F_{\mathrm{bb}}/F_{\mathrm{br, ROSAT}}$	$\sim 170^{(a)}$	$\sim 80^{(b)}$	$\sim 90^{(c)}$

Synthetic cyclotron light curves are derived from the phase-dependent model spectra of the accretion-column *(b)* by folding them with the Johnson and XMM-Newton OM filter bandpasses, and white-dwarf and accretion-stream light curves from model components *c* and *d*. By comparing them with observational data, we determine their respective phase shifts and intensities. As an example, Fig. 2 shows the cyclotron spectra calculated for RS Cae, Fig. 3 the corresponding synthetic *UBVRI* light curves.

Using a consistent set of parameters for all components, we thus establish a physically realistic and consistent multi-wavelength model of the whole binary system, missing only the unknown spectral contribution of the accretion stream. We describe its successful application to the multi-wavelength data of RS Cae in Traulsen et al. (2014). The most relevant limitation relates to the different observational epochs of the high-state data. While we need low-state spectra in the IR and UV to identify the secondary and (unheated)

primary star, all high-state data should be, ideally, observed simultaneously, due to the high variability of the accretion processes.

4 Probing the Accretion Processes in X-Rays

As described above, X-ray data are not the sole, but the main source of information on the accretion mechanisms in magnetic CVs. They give us access to characteristic determinants of the systems and their evolution like mass accretion rate, component masses, and bolometric fluxes / luminosities, which let us distinguish between accretion scenarios like standing or buried shocks or inhomogeneous accretion. These objectives, however, are limited by the complexity of the puzzle and by the energy resolution and signal-to-noise ratio of currently available X-ray data. Several model approaches have been developed, each of them focusing on different aspects, as Cropper et al. (1999, mass determination and effective spectral fitting), Fischer & Beuermann (2001, column structure, SED coverage). Mass and flux determination particularly depend on the underlying spectral models (see also Cropper et al. 1999).
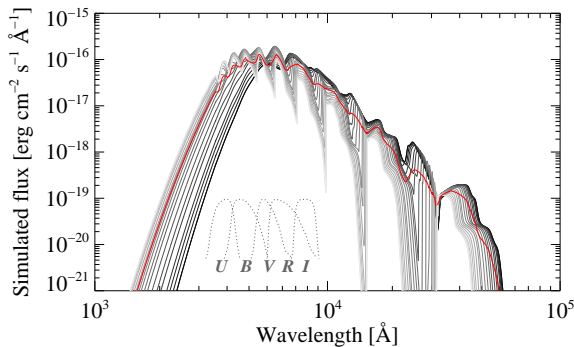

Figure 2: Spectral models of cyclotron emission for $B = 36\,\mathrm{MG}$, $\dot{m} = 0.01$, $1.0\,\mathrm{g\,cm^{-2}\,s^{-1}}$, and the estimated accretion geometry of RS Cae: orbital mean (red) and phase-resolved from $\varphi_{\mathrm{mag}} = 0.0$ (light) to 0.5 (dark). Dotted: Johnson filter bandpasses, used to derive the light curves in Fig. 3.

The X-ray soft component is usually modeled by an absorbed black body, which is on the one hand an appropriate approach for CCD data, not resolving the line features. On the other hand, non-LTE processes and the metal-richness of the hot photosphere have a non-negligible effect on the spectral continuum in the UV to X-rays (cf. Rauch 2003 and references therein). The relevance of consistent non-LTE modeling, considering line-blanketing by heavier elements has been demonstrated for non-accreting hot white dwarfs (e.g. Traulsen et al. 2005). Bolometric fluxes derived from black-body fits to XMM-Newton data are lower by fac-

tors up to five than from non-LTE models, which typically yield lower effective temperatures and hydrogen absorptions. Multi-temperature models, designed to reproduce the temperature gradient in the heated accretion region, result in increased bolometric fluxes by at least $50\,\%$ with respect to single-temperature models. To illustrate the differences between the models, we simulate pointed observations with the upcoming eROSITA mission (Merloni et al. 2012), which will have a higher effective area at energies between 0.2 and $2\,\mathrm{keV}$ than
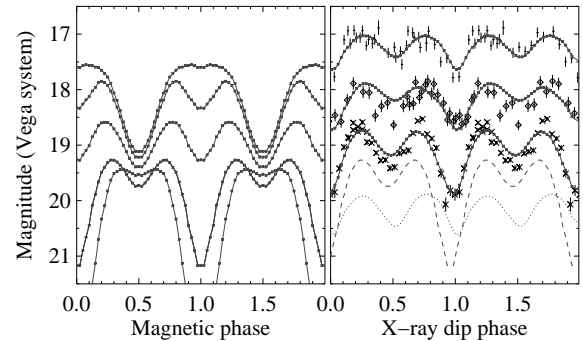

Figure 3: Simulated and observed light curves of RS Cae. *Left: UBVRI* models (bottom to top), derived from the spectra in Fig. 2. *Right:* SMARTS/*B*, XMM-Newton/*U* and UVW1. Dashed: cyclotron emission, dotted: white dwarf and accretion stream.

XMM-Newton and ROSAT. Figure 4 shows $50\,\mathrm{ks}$ eROSITA spectra based on fits to the XMM-Newton data of AI Tri (reduced χ^2 between 0.96 and 1.01).

For the X-ray hard post-shock spectra, we adopt the radiation-hydrodynamic models by Fischer & Beuermann (2001). They are valid for shallow accretion columns, both for the shock scenario dominated by bremsstrahlung cooling and the bombardment scenario dominated by cyclotron cooling. To make them available for automated spectral fitting of X-ray CCD and grating data, we incorporate their temperature and density distributions in XSPEC, using the local mass flow densities $\dot{m}$ and magnetic field strengths B listed in their paper and white-dwarf masses $M_{\mathrm{WD}} = 0.6$, 0.8, and $1.0\,M_\odot$. We parameterize the distributions for 30 layers of a stratified column, and add up 30 APEC plasma components to the final combined column spectrum. Our models include velocity shifts and broadening of the emission lines by stream motion, gravity, orbital motion, and the changing viewing angle. Adding a PEXMON reflection component (Nandra 2007) and multiplying it with the same orbital velocity term, we get a comprehensive description of the phase-dependent emission induced by the accretion column, in particular of the iron lines between 6.4 and $6.9\,\mathrm{keV}$. Figure 5 shows composite accretion-column models compared to

a 50 ks synthetic spectrum of an (illustrative) polar with similar fluxes to AM Her. The models include the same reflection term and different column parameters.

The unabsorbed bolometric fluxes of the column models are typically by about 50 % higher than of the corresponding single-temperature fits. The intrinsic absorption and reflection components have a considerable impact on the fluxes (cf. Cropper et al. 1999), which increase by factors up to 15 compared to pure plasma models. The soft-to-hard flux ratios, thus, may significantly vary for the same object and observation, depending on the model choice.
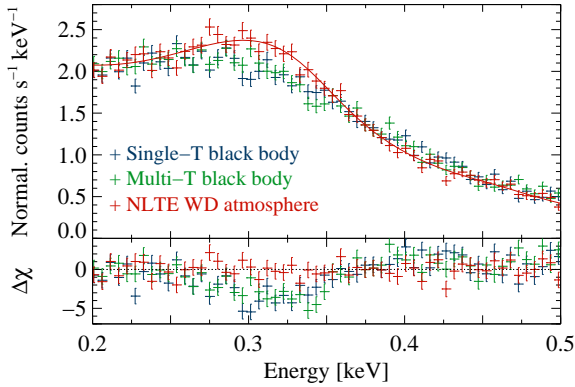

Figure 4: Synthetic spectra of a 50 ks eROSITA pointed observation, based on different models for the heated white dwarf in the X-ray soft polar AI Tri.
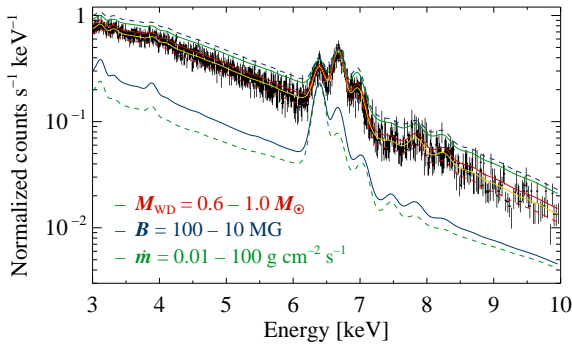

Figure 5: Simulated 50 ks eROSITA observation of a polar at $\dot{m} = 1.0\,\mathrm{g\,cm^{-2}\,s^{-1}}$, $B = 30\,\mathrm{MG}$, $M_{\mathrm{WD}} = 0.8\,M_\odot$, scaled to the XMM-Newton spectrum of AM Her (black: data, yellow: model). Each colored line represents one parameter that is varied while the other parameters and the reflection component are fixed (dashed: lowest, solid: highest value).

5 Conclusions

Our XMM-Newton observations confirm the soft X-ray excess of the three selected polars and indicate inhomogeneous accretion processes. We develop composite models including the contributions of the stellar atmospheres and the X-ray emitting accretion regions for a physically realistic description of the binary system and the accretion processes. Simultaneous multi-λ observations are relevant for a fully consistent SED fitting. The upcoming eROSITA survey will significantly increase the total number of known systems and of systems for that reliable soft-to-hard ratios can be derived. Survey and pointed observations will enable us to better distinguish between different models of the accretion processes, refine them, and push our knowledge about the physical properties of the X-ray emission regions of polars.

References

[1] Burwitz, V. et al.: 1996, A&A 305, 507

[2] Cropper, M. et al.: 1999, MNRAS 306, 684
doi:10.1046/j.1365-8711.1999.02570.x

[3] Fischer, A., Beuermann, K.: 2001, A&A 373, 211

[4] Hauschildt, P. H., Baron, E.: 1999, J. Comp. Appl. Math. 109, 41
doi:10.1016/S0377-0427(99)00153-3

[5] Knigge, C.: 2006, MNRAS 373, 484
doi:10.1111/j.1365-2966.2006.11096.x

[6] Merloni, A. et al.: 2012, arXiv:1209.3114

[7] Nandra, K. et al.: 2007, MNRAS 382, 194
doi:10.1111/j.1365-2966.2007.12331.x

[8] Rauch, T.: 2003, A&A 403, 709

[9] Schwarz, R. et al.: 1998, A&A 338, 465

[10] Schwope, A. D. et al.: 1995, A&A 293, 764

[11] Schwope, A. D. et al.: 2007, A&A 469, 1027

[12] Staude, A., Schwope, A. D., Schwarz, R.: 2001, A&A 374, 588

[13] Townsley, D. M., Gänsicke, B. T.: 2009, A&A 693, 1007

[14] Traulsen, I. et al.: 2005 in 14th European Workshop on White Dwarfs, D. Koester & S. Moehler (eds.), ASP Conf. Ser. 334, 325

[15] Traulsen, I. et al.: 2010, A&A 516, A76

[16] Traulsen, I. et al.: 2011, A&A 529, A116

[17] Traulsen, I. et al.: 2014, A&A 562, A42

[18] Vogel, J. et al.: 2008, A&A 485, 787

[19] Werner, K., Dreizler, S.: 1999, J. Comp. Appl. Math. 109, 65

DISCUSSION

CHRISTIAN KNIGGE: Your data on AI Tri seems to show that the hard X-ray flux actually decreases as the accretion rate (and soft X-rays) increase. What is the interpretation of this?

KLAUS REINSCH: It is related to the response of the accretion shock height to the changing specific accretion rate. In addition, a higher fraction of inhomogeneous accretion events can suppress X-ray hard emission. The first observation of AI Tri during an extremely soft state does not cover a full binary orbit.